



Figure 1: These gem-quality Co-bearing blue spinels (3–12 ct) come from a new deposit in the Lukande area of Tanzania. Composite photo by M. S. Krzemnicki.

Cobalt-bearing Blue Spinel from Lukande, near Mahenge, Tanzania

Michael S. Krzemnicki, Alex Leuenberger and Walter A. Balmer

ABSTRACT: In September 2021, a new deposit of Co-bearing blue spinel was discovered in the Lukande area, south of Mahenge in central Tanzania. We analysed 44 faceted spinels from this source, ranging from Co-dominated blue to Fe-dominated (greyish) blue. Interestingly, nearly all of these spinels showed characteristic inclusion features, consisting predominantly of oriented rhombic lamellae (inferred to be högbomite), as well as oriented short needles and particles. In addition, trace-element analyses revealed two types of spinel from this new deposit: attractive blue stones that showed an average Co concentration of 32 ppm (designated type I), and darker material with distinctly higher Co (averaging 200 ppm; designated type II). The latter showed a beautiful blue colour only when cut into melee-sized stones (i.e. about 2 mm diameter). Based on their trace-element composition, stones from this new deposit near Lukande can be separated from Co-bearing spinels from Vietnam, Sri Lanka and Pakistan. U-Pb dating of surface-reaching zircon inclusions indicates the Tanzanian spinels formed during a late stage of the East African Orogeny, possibly overprinted by the Kuunga-Malagasy orogeny (about 500–570 million years ago).

The Journal of Gemmology, 38(5), 2023, pp. 474–493, <https://doi.org/10.15506/JoG.2023.38.5.474>
© 2023 Gem-A (The Gemmological Association of Great Britain)

Gem-quality spinel (MgAl_2O_4) from Tanzania has been well known in the trade for many decades. However, until recently, fine blue Co-bearing spinel (e.g. Figure 1) was quite rare from this country. Gem-quality Tanzanian spinel was described from the Uмба Valley (near the Kenyan border), and later from the Uluguru Mountains near

Morogoro in the central part of the country. These spinels were mostly red to pink and purple (Bank *et al.* 1989; Hänni & Schmetzer 1991; Schmetzer & Berger 1992). Occasionally, blue spinel from the Morogoro Region has been mentioned in the literature (Schmetzer & Berger 1992) and, later, was found together with other gem varieties in alluvial deposits at Tunduru in

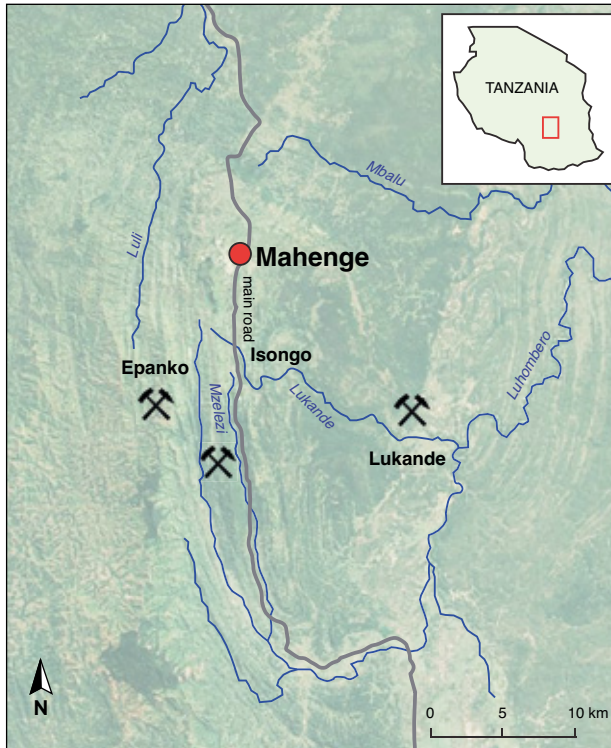


Figure 2: The locations of the spinel deposits at Epanko, Isongo and Lukande in the Mahenge area of central Tanzania are shown on this map (slightly adapted from Hendy *et al.* 2018 and combined with a background image from Google Earth).

southern Tanzania (Henn & Milisenda 1997; Schaub 2004; D'Ippolito *et al.* 2015; Sokolov *et al.* 2019).

Since the 1990s, spinel (together with ruby) has also been found in the Mahenge Mountains near the township of Mahenge in south-central Tanzania (Figure 2), but in rather limited quantities (Koivula *et al.* 1993; Quinn & Laurs 2004; Kukharuk & Manna 2019). This dramatically changed in August 2007 with the discovery of several giant (up to 54 kg) pinkish red crystals at Epanko (or Ipanko), located several kilometres south-west of Mahenge (Weinberg 2007; Pardieu & Hughes 2008). Several gemstones of exceptional quality and size (10–50 ct) were cut from this material, placing these Tanzanian spinels among the most sought-after gems in the international trade. During a visit to the Epanko spinel deposits in October 2009, two of the authors (WAB and MSK) also visited small artisanal mining sites for purple and greyish violet Fe-rich spinels about 5 km south of Isongo village near Mahenge.

To the authors' knowledge, until recently, Co-bearing blue spinel from Tanzania was known only from Tunduru, where a very few vivid blue stones have been mined. However, in September 2021, a new deposit of Co-bearing blue spinel was discovered near Lukande, which is located about 15 km south-east of Mahenge.

The attractive colouration and availability of relatively large sizes (again, see Figure 1) have generated significant interest in this spinel in the gem trade (Branstrator 2022; Krzemnicki 2022; Stephan *et al.* 2022). In this article, we describe this new material and its gemmological characteristics.

LOCATION AND MINING

The new deposit of Co-bearing blue spinel is located near Lukande village (8°48'40.0" S, 36°50'00.0" E; Figure 2), which is a 45-minute drive on a dirt road from Mahenge. The mining area is situated in a valley with farmland, near a site where rubies were dug in the 1990s (i.e. at the 'Simba' mine). The spinel occurs in an eluvial layer buried approximately 1–8 m below the surface, together with other minerals of little commercial value (mostly ruby and pink sapphire of low quality). Artisanal miners use simple tools such as shovels to remove the overburden (dark-coloured soil; Figure 3). The spinels are also mined from heavily weathered marble, which has partially decomposed into soil (Figure 4). The miners load the gem-bearing material into bags, which are carried on bicycles to a nearby stream, where washing is done using sieves (Figure 5). Larger-sized stones are found in big blocks of unweathered marble, which miners break using hammers.

One of the authors (AL) visited the mining area in January 2022, when about 3,000 people were working there. About 300–500 of them were reportedly from Mahenge, but most came from elsewhere in Tanzania and even neighbouring countries such as Mozambique, Kenya and Burundi. In response to the initial mining rush, local government supervisors divided the area into small mining plots of about 6 × 10 m, which the



Figure 3: Artisanal miners search for blue spinel in a series of pits near Lukande. Photo by A. Leuenberger.



Figure 4: A pile of soil from weathered marble will be taken to a nearby stream for washing Co-bearing spinel. Marble boulders are also visible in this pit. Photo by A. Leuenberger.

artisanal miners could work after paying a fee equivalent to USD10 to compensate the landowners. Access to the mines by foreigners and gem dealers is generally restricted; only local brokers can buy stones from the miners (Figure 6), and they must present the gems to government officials at the mining office in Mahenge. The brokers are then required to pay a royalty upon selling the rough material to local dealers and foreign buyers.

According to information gathered during author AL's visit to the area in January 2022, most miners are unable to cover their mining expenses, partly because the spinels are commonly included and tend to have an undesirable greyish purple, greyish blue or greenish blue colouration. The production of attractive facetable blue-coloured Co-bearing spinel from this deposit is

rather small, and as of March 2022 only several hundred rough stones had been found that could yield clean blue gemstones up to 3 ct (e.g. Figure 7). Faceted stones of fine quality over 5 ct are rare. Of the approximately 50 blue spinels from this deposit analysed so far by SSEF, only a few exceptional stones weighed 10+ ct.

The miners also find some very dark to nearly black rough spinel (e.g. bottom left in Figure 7). Since faceting this material in typical gem sizes would yield over-dark stones, it is cut into small gems (usually calibrated melee sizes) to reveal a beautiful Co-related blue colour (Figure 8).

Most of the blue spinels from this new deposit first came to the Sri Lankan market, and subsequently they have been popular with Chinese buyers working in Bangkok, Thailand. A small number of these faceted spinels were offered at the February 2022 Tucson shows, mostly in 2–3 ct sizes. So far in 2023, the authors estimate that a few hundred of these blue spinels have been shown at various trade shows. The majority weighed 1.5–3.5 ct, while larger sizes up to 7 ct were uncommon and good-quality stones exceeding 10 ct were rare.

GEOLOGY

Similar to other marble-related spinel and ruby deposits in East Africa, the Co-bearing spinel deposit near Lukande is related to the Neoproterozoic East African Orogeny (EAO). This large-scale mountain-building event occurred when parts of East and West Gondwana collided about 640–580 million years (Ma) ago, and eventually led to the formation of large, high-grade metamorphic complexes in today's East Africa (i.e. the



Figure 5: Spinel miners use sieves to wash gem-bearing gravel in a local stream. Photo by A. Leuenberger.



Mozambique Metamorphic Belt; Stern 1994; Meert 2003; Fritz *et al.* 2005; Hauzenberger *et al.* 2007 and references therein). Rocks of the EAO include two granulitic terrains in Tanzania: the Western and Eastern Granulites. The Eastern Granulites, which host the spinel deposits near the municipalities of both Morogoro and Mahenge, consist of a migmatitic basement of juvenile crustal and meta-igneous rocks which are overlain by



Figure 7: These Co-bearing spinels (about 1–4 g each) from the Lukande area were offered for sale by a local gem broker in Arusha, Tanzania. They were collected over four weeks during the most intense mining period in November 2022. The very dark stones at bottom-left can be cut into melee-size stones to reveal their blue colour (see Figure 8). Photo by A. Leuenberger.

a cover sequence of metamorphosed sedimentary units containing gem-bearing marble units (Möller *et al.* 2000; Fritz *et al.* 2005; Hauzenberger *et al.* 2007 and references therein). The initial sedimentation of the metacarbonate cover sequence took place in close proximity to the hinterland, most probably during the early Neoproterozoic. A lagoon or lacustrine sediment basin on the passive continental margin of former East Gondwana seems to be a plausible geological setting (Balmer *et al.* 2017).

During the EAO, a high-grade metamorphic event (amphibolite-to-granulite facies conditions) led to the formation of the gem deposits within the cover sequence of the Eastern Granulites. These include the ruby and spinel occurrences in the Mahenge Mountains and Uluguru Mountains. Finally, the gem-bearing marbles of



Figure 8: Five small calibrated spinels (from left to right: SPTan-2_1 to SPTan-2_5; each approximately 2 mm diameter; total weight 0.17 ct), reportedly cut from very dark rough from the same mining area near Lukande, were examined for this study. Photo by Alice Chalain, SSEF.

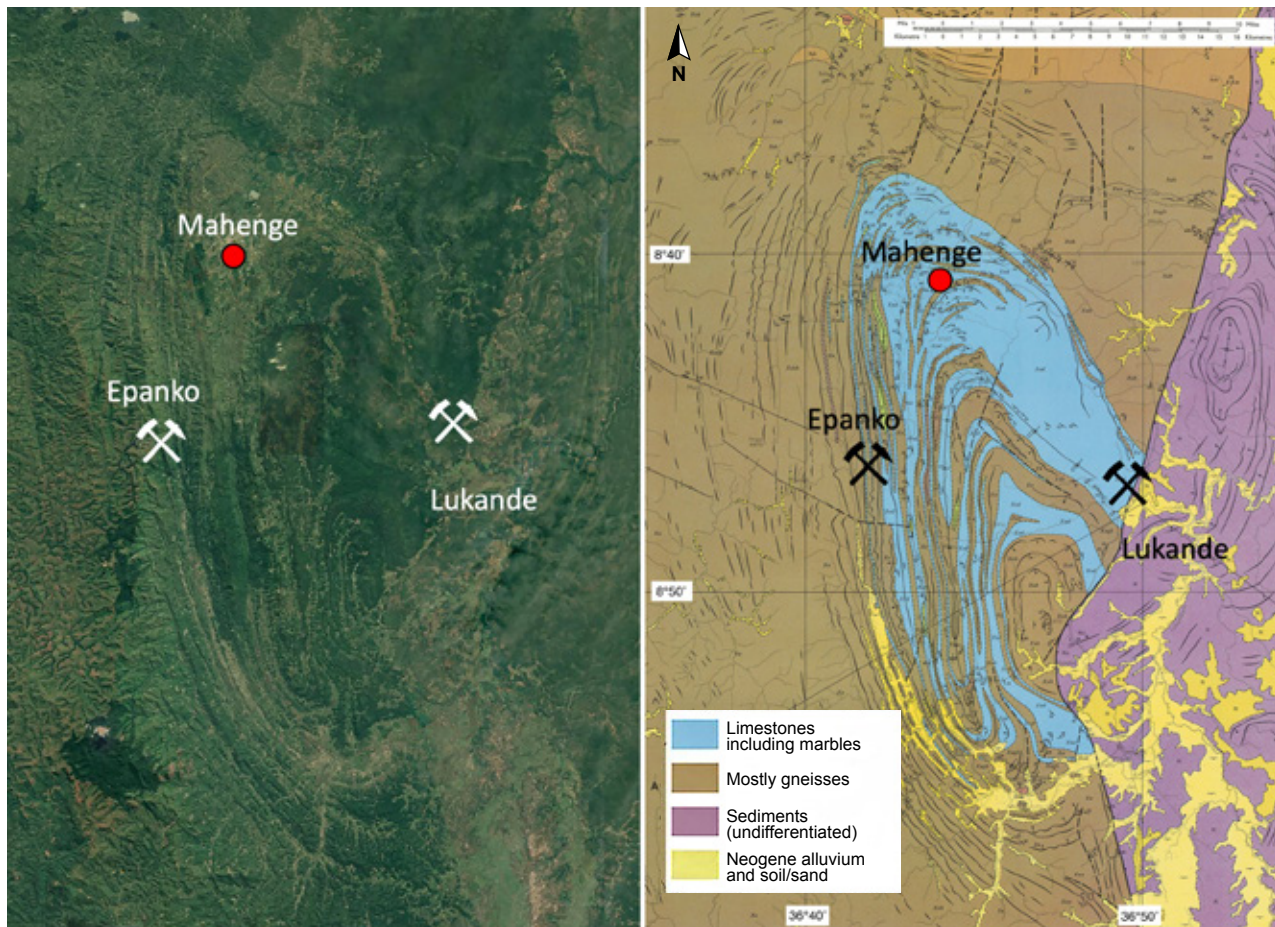


Figure 9: Both a satellite image (from Google Earth) and geological map (from Birch & Stephenson 1962) of the Mahenge Mountains show the folded nappe structure that covers an area about 35 km long and about 20 km wide. Pink-to-red spinel is mined at Epanko, and the new deposit of Co-bearing blue spinel is located near Lukande.

the Morogoro Region were affected by greenschist-facies metamorphism, which is linked to the Kuunga-Malagasy orogen (about 500–570 Ma), a late-stage episode of the EAO (Balmer 2011; Fritz *et al.* 2013; Balmer *et al.* 2017). Structurally, the gem-bearing marbles form regional nappes (thrust sheets) overlaying the granulitic basement gneisses (Figure 9). These nappes were thrust onto the basement in a north-western direction. The nappe structures are cross-cut in their root zones by a major fault with a mostly north-eastern-trending strike (Birch & Stephenson 1962; Sampson & Wright 1964; Schlüter 1997; Rossetti *et al.* 2008; Fritz *et al.* 2009; Balmer *et al.* 2017). The Co-bearing spinel deposit near Lukande is located in the root zone of the local nappe structure in the Mahenge Mountains.

Since the host rock at Lukande is strongly weathered, a detailed petrographic characterisation (e.g. marble or calc-silicate-rich metacarbonate) has not been possible. Still, what was observed on site by author AL appears to relate well to other marble-hosted spinel deposits in the Mahenge Mountains (examined previously by

author WAB; see Balmer *et al.* 2017), as well as at additional localities where Co-bearing spinel is found as an accessory mineral in marble or other metacarbonates, such as in Vietnam (Chauviré *et al.* 2015), Canada (Belley & Groat 2019), Tajikistan (Schwarz *et al.* 2022) and Pakistan (Schollenbruch *et al.* 2021).

MATERIALS AND METHODS

The Lukande spinels analysed for this study were kindly provided by several reliable gem dealers (e.g. in Arusha, Tanzania). They mainly consisted of 39 faceted stones ranging from 2.07 to 11.25 ct, most of which had an attractive blue colour and fine clarity (e.g. Figures 1 and 10). The study sample also included five calibrated melee-sized vivid blue spinels (total weight 0.17 ct; Figure 8) that were cut from very dark rough material reportedly found in the same area (S. Jaquith, pers. comm. 2023). Based on differences in the colour and trace-element composition (as reported below) for these two groups, we separated them into two categories,

with the main ones designated type I (sample numbers starting with SPTan-1) and the melee stones as type II (SPTan-2); all of them are listed in Table I.

The samples were characterised with standard gemmological instruments (i.e. refractometer, hydrostatic balance, and long- and short-wave UV lamps), except for the type II spinels, for which RI and SG values were not determined due to their small size. Internal features in all stones were examined with a System Eickhorst Gemmaster microscope with Zeiss optics.

Ultraviolet-visible-near infrared (UV-Vis-NIR) absorption spectroscopy was performed on all type I samples and one type II spinel using a Cary 500 spectrophotometer in unpolarised mode (290–900 nm range with 1 nm resolution).

For inclusion identification and photoluminescence (PL) spectroscopy, we used a Renishaw inVia Raman microscope with an argon laser (514 nm emission). Raman analyses of inclusions in selected samples were done with 20× or 50× magnification, using a spectral resolution of 1.6 cm⁻¹ in the range of 150–1400 cm⁻¹ Raman shift (or 150–1800 cm⁻¹ for zircon) with a 10 s counting time. To increase the signal-to-noise ratio, spectra were accumulated 3–10 times depending on the quality of the signal. For PL spectroscopy, only a single scan was measured in the 600–800 nm range.

Chemical analyses were performed by energy-dispersive X-ray fluorescence (EDXRF) spectroscopy with a Thermo Quant’X instrument using our in-house-developed spinel setup with excitation energies ranging from 4 to 25 kV. All type I samples were analysed, but not the type II spinels due to their small size. In addition, trace- and ultra-trace-element analyses were carried out on 17 type I samples (specified in Table I) and all five type II spinels with our GemTOF system (laser ablation inductively coupled plasma time-of-flight mass spectrometry; LA-ICP-TOF-MS) using a 193 nm ArF excimer laser with a fluence of 5.6 J/cm². For each sample, we analysed three to four spots (usually on the girdle) that were each 100 µm diameter. Reference glass NIST SRM 610 was used as the external standard and the theoretical (stoichiometric) Al concentration of spinel as the internal standard. By using a time-of-flight (TOF) system, we were able to record nearly all elements in the periodic table simultaneously at ultra-high speed and high sensitivity. The limit of detection of our TOF-MS setup ranges from single-digit-ppb for heavy elements to low-ppm for light elements. The error bars (uncertainty) for each data point in the LA-ICP-MS plots were calculated using the transient signal and found to be commonly about 1–2%—distinctly smaller than the

data points in the logarithmic diagrams presented in this article. The same instrumentation was used for the radiometric dating of a total of four surface-reaching zircon inclusions in two of the spinel samples (SPTan-1_3 and SPTan-1_13). More detailed information about this highly versatile system, and the analytical settings used for the chemical analyses and radiometric dating, can be found in Wang *et al.* (2016), Phyo *et al.* (2020) and Wang and Krzemnicki (2021).

RESULTS

Gemmological Properties

The samples showed an attractive blue colour, ranging from blue to slightly greyish blue to greenish blue, often with vivid blue internal reflections. In addition, many of the stones showed high clarity, even in large sizes (e.g. Figure 10).

The type I spinels had an RI ranging from 1.712 to 1.718 and an SG of 3.59 to 3.62, consistent with the expected values for Mg-Al spinel. Although the RI and SG values of the five type II melee samples could not be measured with acceptable accuracy, we would expect them to be slightly higher due to their trace-element composition (see below). Most of the investigated spinels showed a weak greenish reaction when exposed to long-wave UV radiation, but were inert to short-wave UV.

Microscopic Features

All of the samples contained some inclusions. Regularly arranged rhombic (to slightly irregular) lamellae oriented parallel to the octahedral crystal directions were among the most prominent features (see also Table I). They often showed intriguing iridescence colours when rotated under a light source (Figure 11). They



Figure 10: This 7.48 ct Co-bearing spinel (SPTan-1_31) from the Lukande area was cut from one of the larger pieces of rough in Figure 7. Photo by Luc Phan, SSEF.

Table I: Tanzanian Co-bearing spinel samples characterised in this study.


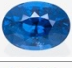







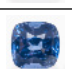
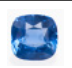



























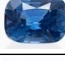


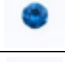


Photo	Sample	Weight (ct)	Shape	RI	SG	Microscopy (main features)	GemTOF	PL band at 640 nm
	SPTan-1_1	3.13	Cushion	1.715	3.61	Högbomite lamellae, apatite, zircon	Yes	Distinct
	SPTan-1_2	10.68	Oval	1.718	3.62	Högbomite lamellae, etc. ^a	Yes	Distinct
	SPTan-1_3 ^b	10.62	Cushion	1.716	3.60	Högbomite lamellae, zircon, apatite, mica	Yes	Moderate
	SPTan-1_4	8.67	Oval	1.714	3.61	Högbomite lamellae, etc.	Yes	Distinct
	SPTan-1_5	6.78	Cushion	1.714	3.59	Högbomite lamellae, etc.	Yes	Distinct
	SPTan-1_6	3.55	Cushion	1.715	3.60	Högbomite lamellae, apatite	Yes	Distinct
	SPTan-1_7	2.77	Cushion	1.712	3.60	Particles, zircon	Yes	Moderate
	SPTan-1_8	2.64	Oval	1.714	3.60	Högbomite lamellae, etc.	Yes	Distinct
	SPTan-1_9	2.52	Cushion	1.714	3.62	Högbomite lamellae, etc.	Yes	Distinct
	SPTan-1_10	2.30	Cushion	1.714	3.61	Högbomite lamellae, etc.	Yes	Moderate
	SPTan-1_11	2.28	Cushion	1.712	3.59	Högbomite lamellae, etc.	Yes	Distinct
	SPTan-1_12	2.11	Cushion	1.716	3.62	Högbomite lamellae, etc.	Yes	Weak
	SPTan-1_13 ^c	2.07	Cushion	1.715	3.60	Högbomite lamellae, zircon	Yes	Distinct
	SPTan-1_14	4.46	Cushion	1.715	3.62	Dispersed particles	No	Distinct
	SPTan-1_15	3.31	Oval	1.715	3.61	Högbomite lamellae, etc.	No	None
	SPTan-1_16	4.09	Cushion	1.718	3.61	Dispersed particles	Yes	Distinct
	SPTan-1_17	4.01	Cushion	1.717	3.62	Högbomite lamellae, etc.	No	Distinct
	SPTan-1_18	5.86	Cushion	1.716	3.60	Högbomite lamellae, etc.	No	Moderate
	SPTan-1_19	4.65	Octagonal	1.715	3.60	Högbomite lamellae, etc.	No	Moderate
	SPTan-1_20	4.23	Cushion	1.716	3.60	Högbomite lamellae, etc.	No	Distinct
	SPTan-1_21	3.75	Cushion	1.718	3.61	Högbomite lamellae, etc.	No	Moderate
	SPTan-1_22	5.15	Cushion	1.718	3.62	Högbomite lamellae, etc.	No	Moderate
	SPTan-1_23	5.18	Cushion	1.717	3.62	Högbomite lamellae, etc.	Yes	None
	SPTan-1_24	4.94	Cushion	1.716	3.59	Milkiness	Yes	Moderate

Table I: (continued)

Photo	Sample	Weight (ct)	Shape	RI	SG	Microscopy (main features)	GemTOF	PL band at 640 nm
	SPTan-1_25	4.11	Cushion	1.716	3.62	Högbomite lamellae, etc.	Yes	Distinct
	SPTan-1_26	6.14	Cushion	1.716	3.59	Högbomite lamellae, etc.	No	Distinct
	SPTan-1_27	10.14	Cushion	1.716	3.61	Högbomite lamellae, etc.	No	Distinct
	SPTan-1_28	4.98	Cushion	1.716	3.62	Högbomite lamellae, etc.	No	Distinct
	SPTan-1_29	10.31	Cushion	1.716	3.60	Högbomite lamellae, etc.	No	Distinct
	SPTan-1_30	7.12	Cushion	1.715	3.61	Högbomite lamellae, etc.	No	Moderate
	SPTan-1_31	7.48	Oval	1.715	3.61	Högbomite lamellae, etc.	No	Distinct
	SPTan-1_32	10.07	Cushion	1.714	3.59	Högbomite lamellae, etc.	No	Distinct
	SPTan-1_33	3.54	Heart-shaped	1.717	3.62	Högbomite lamellae, etc.	No	Moderate
	SPTan-1_34	6.66	Cushion	1.717	3.62	Lines of particles, etc.	No	Distinct
	SPTan-1_35	11.25	Cushion	1.715	3.61	Högbomite lamellae, etc.	No	None
	SPTan-1_36	5.52	Oval	1.716	3.60	Högbomite lamellae, etc.	No	nd
	SPTan-1_37	7.13	Cushion	1.717	3.61	Högbomite lamellae, etc.	No	Moderate
	SPTan-1_38	7.09	Cushion	1.718	3.61	Högbomite lamellae, etc.	No	nd
	SPTan-1_39	3.10	Cushion	1.717	3.59	Högbomite lamellae, etc.	No	nd
	SPTan-2_1	0.035	Round	nd	nd	Högbomite lamellae, etc.	Yes	None
	SPTan-2_2	0.038	Round	nd	nd	Högbomite lamellae, etc.	Yes	Moderate
	SPTan-2_3	0.034	Round	nd	nd	Högbomite lamellae, etc.	Yes	Strong
	SPTan-2_4	0.035	Round	nd	nd	Högbomite lamellae, etc.	Yes	Strong
	SPTan-2_5	0.031	Round	nd	nd	Högbomite lamellae, etc.	Yes	Very strong

^a Abbreviations: nd = not determined; etc. = one or more of the following: dispersed fine particles, needles, zones of turbidity, octahedral negative crystals, fissures and partially healed fissures.

^b U-Pb age dating of two zircon inclusions yielded an age of 508 ± 48 million years.

^c U-Pb age dating of two zircon inclusions yielded an age of 501 ± 29 million years.

were first described by Schmetzer and Berger (1992) in reddish to purple spinel from Morogoro, Tanzania, and identified as högbomite, $(\text{Mg,Fe})_2(\text{Al,Ti})_5\text{O}_{10}$. Such inclusions have also been documented in Co-bearing

spinel from Pakistan (Schollenbruch *et al.* 2021), and recently were reported in material from this new deposit in Tanzania (Krzemnicki 2022; Stephan *et al.* 2022).

Our samples occasionally contained various solid

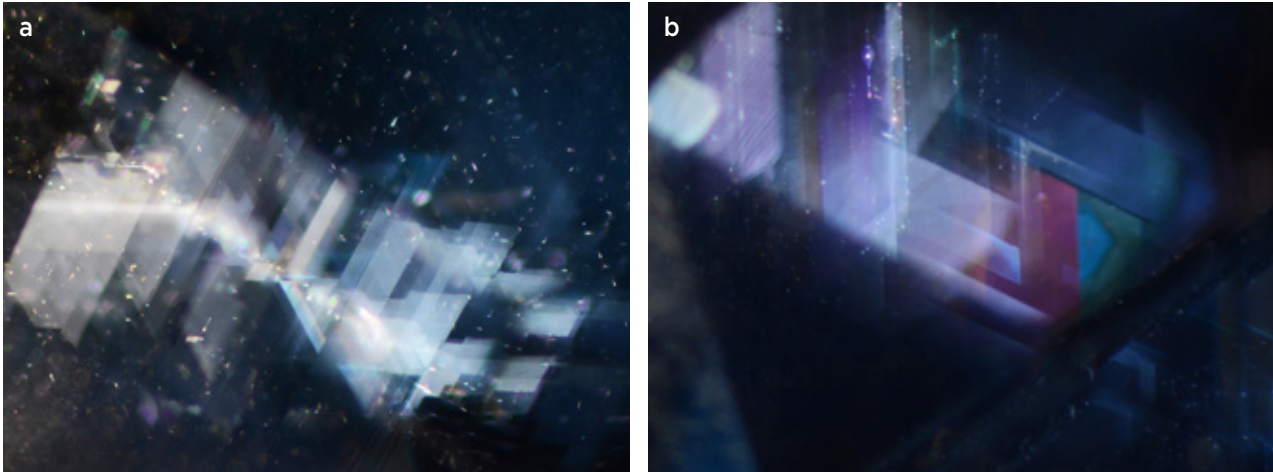


Figure 11: (a) Oriented lamellae in Lukande spinel are inferred to consist of högbomite (magnified 40×). (b) They display iridescence at certain orientations (magnification 70×). Photomicrographs by M. S. Krzemnicki, in darkfield illumination.

inclusions—rounded apatite, phlogopite and zircon—mostly as small clusters (Figure 12). The identity of these three inclusion minerals was confirmed by Raman spectroscopy (Figure 13). The main Raman peak in the zircon spectrum, $\nu_3(\text{SiO}_4)$ at about 1007 cm^{-1} , showed some broadening (FWHM 11.43 cm^{-1}) due to incipient metamictisation (Nasdala *et al.* 1995).

In addition, we commonly observed oriented needle-like inclusions, similar to those reported in blue spinels from Sri Lanka and Vietnam (Shigley & Stockton 1984; Smith *et al.* 2008), and some samples contained zones of milky turbidity caused by minute particles (Figure 14). Also seen were partially healed fissures and octahedral negative crystals, often surrounded by oriented, dotted, discoid structures, resembling to those commonly observed in spinel (e.g. Shigley & Stockton 1984).

UV-Vis-NIR Absorption Spectroscopy

Figure 15 shows UV-Vis-NIR absorption spectra for three samples representing the spectral variation observed in

blue spinel from the Lukande deposit. Band attribution is according to D'Ippolito *et al.* (2015, and references therein), and a brief background on blue spinel colouration is presented in Box A. In general, all the spectra reveal a strong UV-edge absorption due to Fe, and a series of partially overlapping Co and Fe bands in the visible range. The top spectrum in Figure 15 of a greyish-greenish blue sample is dominated by Fe-related absorption bands and has only a limited contribution by Co. The other two spectra (from purer blue samples) exhibit stronger Co-related absorption bands in the visible range. The Co-Fe-related spectral variations of these selected samples is also reflected in their blue to vivid blue colouration. Apart from the presence of Co, the total amount of Fe (which affects the UV absorption edge via $\text{O}^{2-}\text{-Fe}^{2+}$ ligand-metal charge transfer), as well as octahedrally coordinated Fe^{2+} and Fe^{3+} (resulting in an intervalence charge transfer via $\text{Fe}^{2+}\text{-Fe}^{3+}$), both have a major effect on colour, causing the indigo blue colouration to shift to a distinctly more greenish blue (again, see Figure 15).

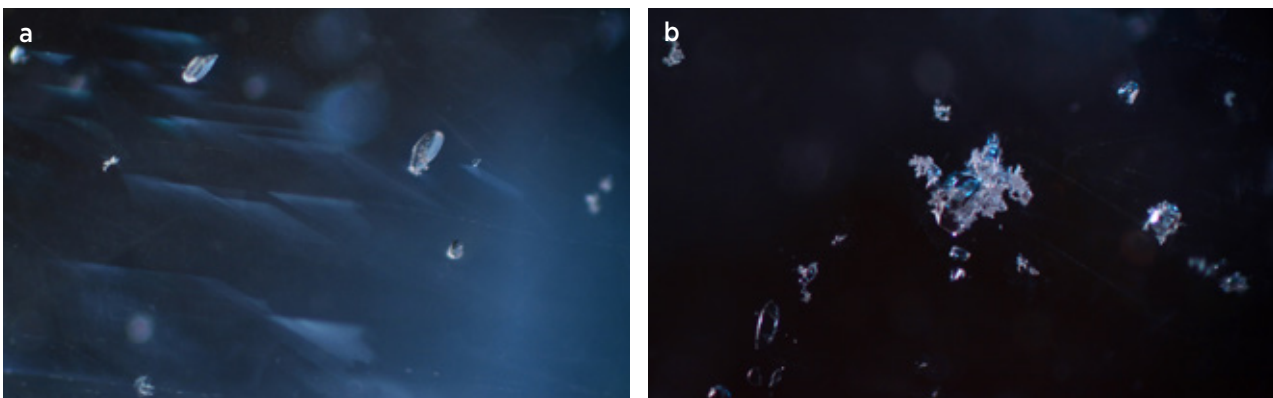


Figure 12: These inclusions in Lukande spinel consist of (a) dispersed apatite crystals and (b) a zircon cluster. Photomicrographs by M. S. Krzemnicki; magnified 50×.

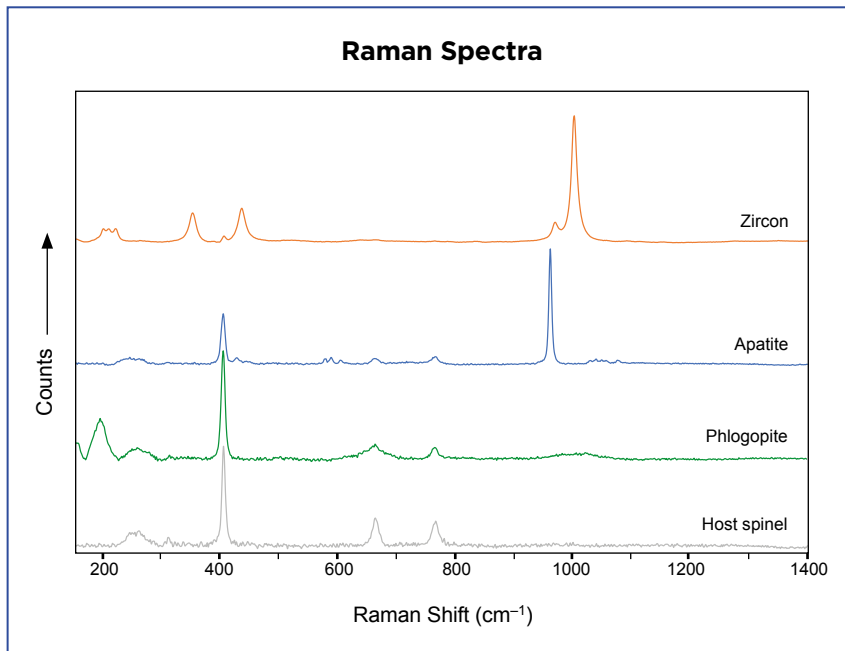


Figure 13: Raman spectra of solid inclusions in the studied spinels from Lukande confirm the presence of zircon, apatite and phlogopite. All spectra were baseline-corrected and are offset vertically for clarity. The zircon peak at about 1007 cm^{-1} shows some broadening due to incipient metamictisation. Peaks from the host spinel (bottom trace) are present to varying degrees in the inclusion spectra.

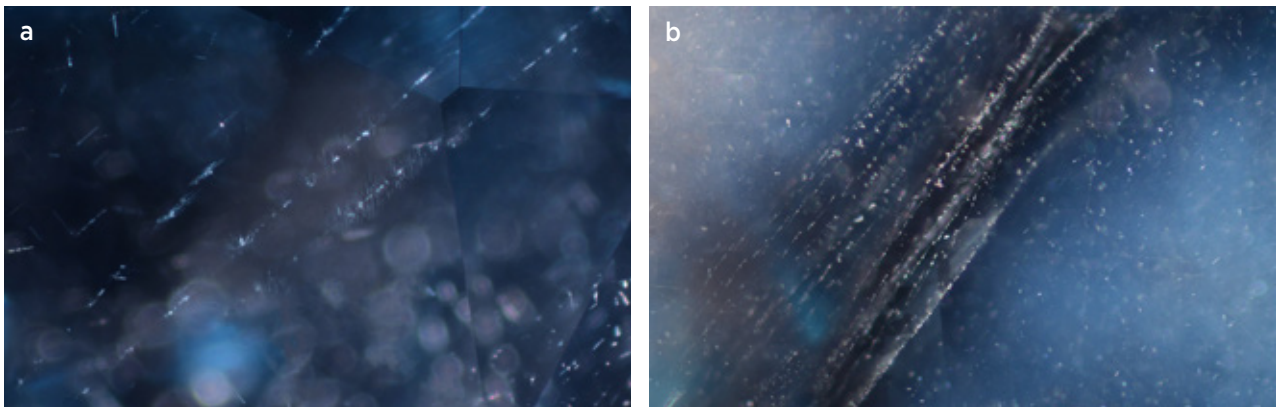


Figure 14: Also present in the Lukande spinels are (a) oriented needles and (b) milky turbidity. Photomicrographs by M. S. Krzemnicki; magnified 40 \times .

Box A: Blue Spinel Colouration

The colour of spinel and, specifically, of Co-bearing blue spinel, has been investigated quite extensively in the literature (e.g. Gaffney 1973; Shigley & Stockton 1984; Schmetzer *et al.* 1989; Hålenius *et al.* 2002; Taran *et al.* 2005, 2009; Bosi *et al.* 2012; Hanser 2013; Fregola *et al.* 2014; Chauviré *et al.* 2015; D'Ippolito *et al.* 2015; Andreozzi *et al.* 2018). Usually, spinel colouration is due to a combination of transition metals—for blue spinel mainly Fe and Co (if present), and in some purplish blue stones also Cr (Schollenbruch *et al.* 2021). Shigley & Stockton (1984) were the first to attribute Co in addition to Fe as an important chromophore in natural blue spinel.

The hue and saturation of the blue colour is not only related to the concentration of the chromophores Fe and Co, but also to the valence state of iron (Fe^{2+} or Fe^{3+}) and their distribution on the two crystallographic sites in the spinel structure.¹ Notably, very low traces of Co have a strong effect on the blue colour of spinel when present as tetrahedrally coordinated Co^{2+} (Marfunin 1979; Schmetzer *et al.* 1989; D'Ippolito *et al.* 2015; Andreozzi *et al.* 2018). Often the amount of Co is so low that it is near the detection limit of EDXRF spectroscopy, which is the technique commonly used to analyse the chemical composition of gem materials in gemmological laboratories.

¹ Designated AB_2O_4 , with A referring to bivalent ions that are generally at the tetrahedrally coordinated T-site (e.g. ${}^{\text{T}}\text{Mg}^{2+}$, ${}^{\text{T}}\text{Fe}^{2+}$ and ${}^{\text{T}}\text{Co}^{2+}$), and B indicating trivalent ions that are typically at the octahedrally coordinated M-site (e.g. ${}^{\text{M}}\text{Al}^{3+}$, ${}^{\text{M}}\text{Fe}^{3+}$ and ${}^{\text{M}}\text{Cr}^{3+}$).

UV-Vis-NIR Spectra

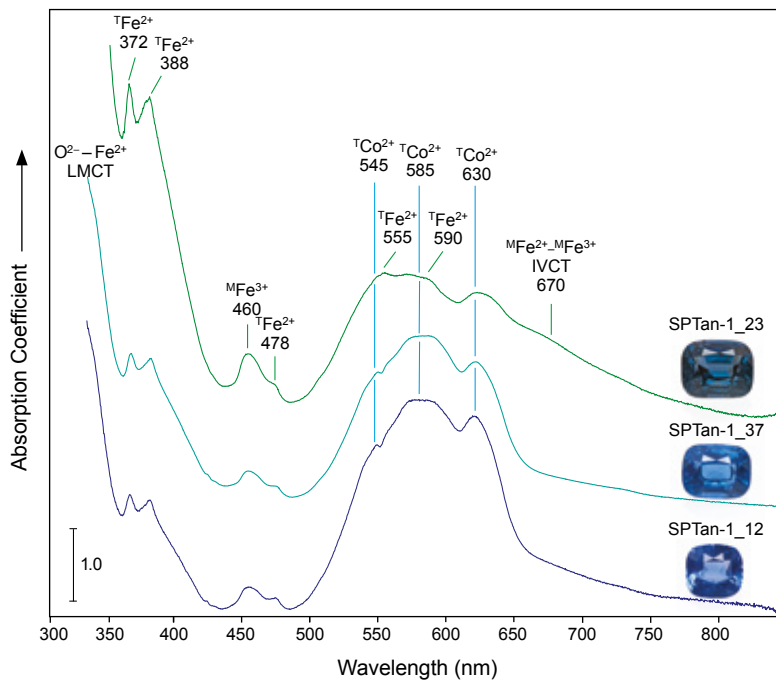


Figure 15: The UV-Vis-NIR absorption spectra of Co-bearing blue spinels from Lukande range from Fe dominated (SPTan-1_23) to Co dominated (SPTan-1_37 and SPTan-1_12). The three spectra have been offset vertically for clarity and corrected for path length (absorption coefficient). Abbreviations: LMCT = ligand-metal charge transfer and IVCT = intervalence charge transfer.

PL Spectra

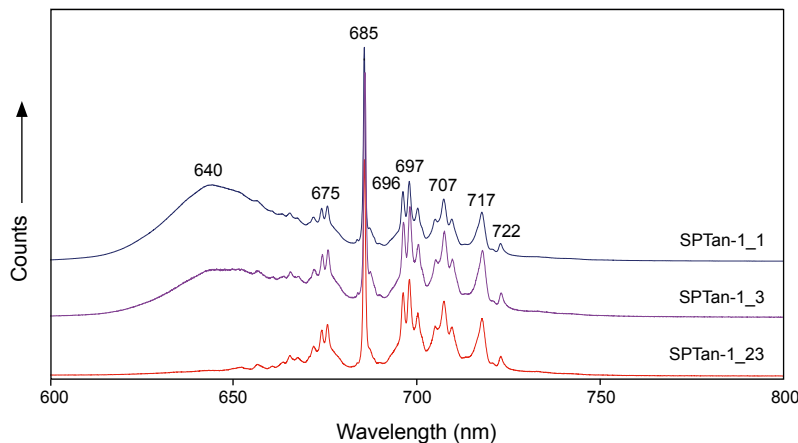


Figure 16: Photoluminescence spectra with 514 nm laser excitation of three representative Co-bearing blue spinels from the Lukande area show a series of PL peaks related to octahedrally coordinated Cr^{3+} and, to a variable extent, a broad band at about 640 nm assumed to be related to octahedrally coordinated Mn^{2+} . The spectra have been offset vertically for clarity.

Photoluminescence Spectroscopy

The PL spectra of the Lukande spinels show a series of emission lines (a so-called organ-pipe spectrum; Figure 16) related to the presence of traces of Cr^{3+} replacing Al^{3+} on the octahedrally coordinated site of the spinel structure. The position and shape (i.e. FWHM) of these emission lines confirm that the samples are natural and have not been heated (Saeseaw *et al.* 2009; Smith 2012; Widmer *et al.* 2014).

In addition, most but not all of the investigated

spinel display a broad emission band at about 640 nm (see Table I). In the literature, a similar broad band has been attributed either to tetrahedrally coordinated Co^{2+} (Abritta & Blak 1991; Kuleshov *et al.* 1993; Chauviré *et al.* 2015) or to octahedrally coordinated Mn (Gaft *et al.* 2015; Khaidukov *et al.* 2020). From our trace-element data, an attribution to Co is not evident, as some of the samples with little or no emission also have higher Co concentrations than those with a distinct 640 nm band, even if we take into account that some Co^{2+} could be

located on the octahedrally coordinated site. An attribution to Mn is more likely, as the three spectra in Figure 16 correlate with increasing Mn concentration (from bottom to top) from about 100 ppm to about 250 ppm. In addition, most of our samples displayed weak greenish luminescence when exposed to long-wave UV radiation. This luminescence results from an emission band at about 514 nm attributed to tetrahedrally coordinated Mn^{2+} in the spinel structure (Yu & Lin 1996; Cornu *et al.* 2015; Khaidukov *et al.* 2020). However, other factors (e.g. quenching by Fe) may also play a role in the presence or absence of the 640 nm band.

Chemical Analysis

EDXRF Spectroscopy. EDXRF chemical analyses of the type I study spinels reveal a very uniform chemical composition (see Table II), with a low standard deviation for most elements. The only element showing larger variations is zinc (Zn^{2+}), which commonly replaces magnesium (Mg^{2+}) at the tetrahedral site. This can be seen in a plot of MgO vs ZnO (Figure 17a), which shows a fairly good negative correlation for these two elements.

The Fe concentration in the investigated spinels is quite constant at about 1.2 wt. % Fe_2O_3 and shows no evident negative correlation with Mg (Figure 17b). This indicates that most Fe is present as octahedrally coordinated Fe^{3+} , with only minor amounts as Fe^{2+} in tetrahedral coordination. Nevertheless, the latter plays a major role in the colouring of these blue spinels, in addition to tetrahedrally coordinated Co^{2+} (see Figure 15).

Although considerably affecting the colour (and absorption spectra) of these spinels, Co was found to be present only at or below the detection limit (about 50 ppm)

Table II: EDXRF analyses of 39 type I Co-bearing blue spinels from Lukande, Tanzania.*

Oxide (wt.%)	Range	Average	Std. Dev.
MgO	27.80–29.42	28.60	0.34
Al ₂ O ₃	68.76–69.93	69.47	0.27
TiO ₂	0.006–0.013	0.010	0.002
V ₂ O ₃	bdl–0.015	0.008	0.003
Cr ₂ O ₃	bdl–0.007	0.004	0.002
MnO	0.034–0.063	0.053	0.006
Fe ₂ O ₃	1.06–1.84	1.24	0.18
Co ₂ O ₃	bdl–0.001	0.001	0.000
NiO	0.011–0.024	0.015	0.003
ZnO	0.152–1.403	0.544	0.338
Ga ₂ O ₃	0.014–0.060	0.033	0.013

* Abbreviations: bdl = below detection limit; Std. Dev. = Standard Deviation.

of the EDXRF system using our analytical setup. As mentioned above, this is common for gem-quality Co-bearing spinel, and traces of this element are best quantified by mass spectrometry (LA-ICP-MS).

Although Ni is commonly present as a trace element in Co-bearing spinels, the Ni concentrations indicated by EDXRF appear too high (analytical error assumed), as shown by comparison with our LA-ICP-MS data.

LA-ICP-TOF-MS Analysis. Table III summarises the trace-element data for the 22 Lukande samples analysed for this study, in comparison with data for Co-bearing

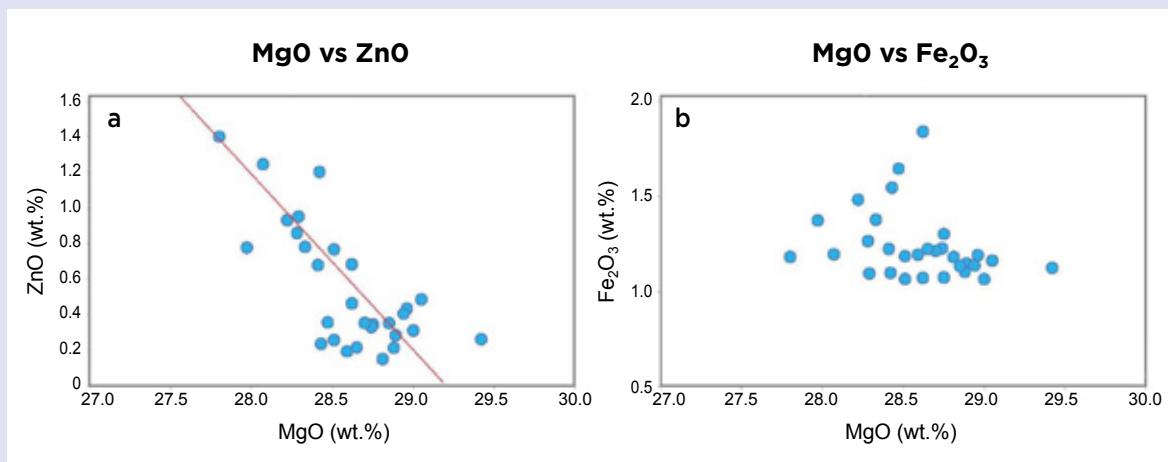


Figure 17: Plots of EDXRF data for the type I Co-bearing spinels show (a) a fairly good negative correlation for MgO and ZnO (red line: $r = -1$), and (b) no such correlation for MgO and Fe_2O_3 .

Table III: Trace-element data for Co-bearing blue spinels from various localities.*

Element (ppmw)	Tanzania, type I (n = 68)			Tanzania, type II (n = 15)		
	Range	Avg.	Std. Dev.	Range	Avg.	Std. Dev.
Li	80.43–318.3	235.0	59.87	102.2–182.9	128.6	29.32
Be	13.82–34.99	20.89	5.02	4.44–12.79	8.75	2.47
Ti	13.33–206.6	36.42	22.17	12.93–75.15	32.67	17.27
V	29.86–78.05	40.78	11.15	58.85–127.8	99.79	23.59
Cr	4.56–129.5	16.17	27.69	7.99–57.15	36.21	15.21
Mn	128.6–293.8	247.0	32.42	44.85–93.32	64.78	16.49
Fe	7242–12850	8940	1474	9295–13960	11800	1890
Co	15.93–48.22	31.74	7.76	88.30–315.0	199.5	86.84
Ni	30.39–58.57	39.77	7.87	80.16–201.8	136.1	44.62
Zn	1007–11540	3855	2854	22370–115890	59493	36194
Ga	81.60–329.7	170.3	73.79	107.0–286.9	166.3	64.23

* Data for Tanzanian, Sri Lankan and Vietnamese samples were obtained at SSEF by LA-ICP-TOF-MS, and data for Pakistani samples were obtained at Gübelin Gem Lab by LA-ICP-MS (courtesy of K. Schollenbruch). Abbreviations: bdl = below detection limit; n = number of points analysed.

blue spinels from Sri Lanka and Vietnam (from the SSEF research database), as well as Pakistan (data obtained from Gübelin Gem Lab). The full trace-element analyses of our Lukande samples are available in *The Journal's* online data depository.

As mentioned above, the Lukande Co-bearing spinels were separated into two categories: type I which shows medium to medium-strong blue colour and can be cut into larger stones (Figure 1), and type II which, as rough fragments, are very dark blue and only display an attractive blue colour when cut into melee sizes of about 2 mm in diameter (Figure 8). These two types not only differ in colour, but also in their trace-element concentrations (see Table III and Figure 18). Type II spinels show, on average, less Mn (about 65 ppm vs about 250 ppm in type I), but distinctly more Co (about 200 ppm vs about 30 ppm in type I) and Ni (about 135 ppm vs about 40 ppm in type I) than the spinels of type I. Iron varies within a limited and similar range in both spinel types. The most obvious difference, however, is the enrichment of Zn (gahnite component) in the type II spinels (up to 115,890 ppmw or 14 wt. % ZnO). Although Zn and other trace elements (e.g. chromophores such as Fe and Co) vary considerably from sample to sample (e.g. from 1,000 to 100,000 ppm Zn), multiple analyses of a single stone show a relatively constant chemical composition (see data in *The Journal's* data depository). This sample homogeneity also applies to spinel from many other origins. This also explains why gem-quality spinels are generally of homogeneous

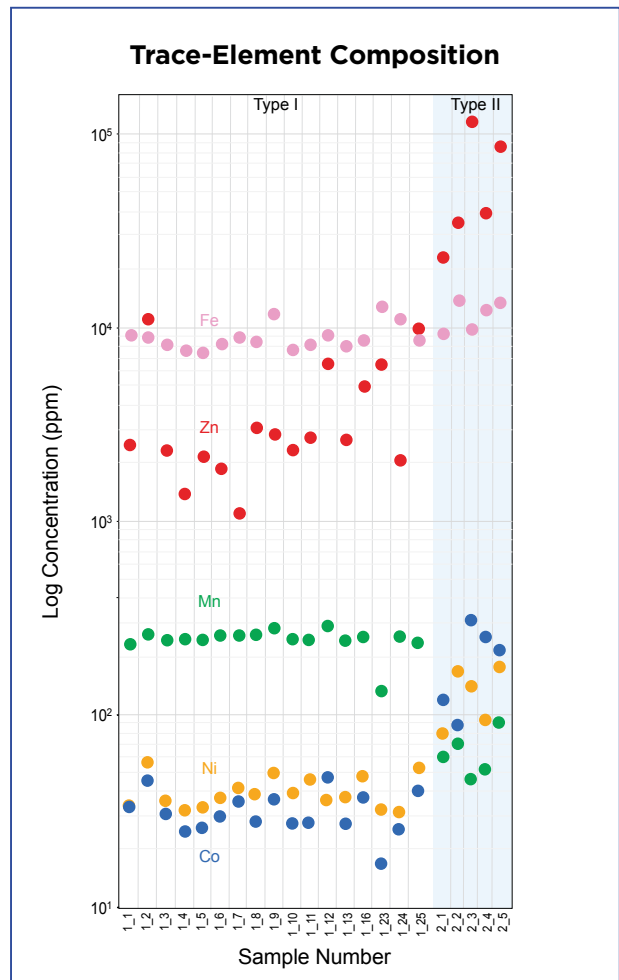


Figure 18: The concentrations of selected trace elements (Fe, Zn, Mn, Ni and Co) are shown for both type I and type II Co-bearing spinels from the Lukande area. Notably, the type I spinels contain much less Zn, Ni and Co—and more Mn—than the type II spinels.

Table III: (continued)

Sri Lanka (n = 20)			Vietnam (n = 33)			Pakistan (n = 103)		
Range	Avg.	Std. Dev.	Range	Avg.	Std. Dev.	Range	Avg.	Std. Dev.
12.32-185.8	95.58	57.71	42.70-859.9	294.5	229.8	7.90-561.2	268.0	149.6
3.97-101.8	46.26	32.35	9.82-72.79	20.17	18.84	11.83-78.04	33.95	14.62
bdl-81.62	20.09	28.44	bdl-8.10	2.04	2.30	3.01-1102	117.4	171.9
11.65-86.09	34.06	24.18	2.10-25.61	8.15	7.63	49.56-917.8	190.2	159.7
0.296-20.85	6.84	8.22	0.96-76.66	13.38	25.70	108.2-4947	1142	946.3
26.51-619.9	272.4	223.9	49.14-289.1	120.4	78.66	32.48-192.6	85.48	45.85
5523-23560	15310	6039	3758-21980	14030	6030	10110-47170	20820	10140
17.33-109.9	54.23	29.80	10.82-71.94	39.95	17.84	62.36-420.5	226.6	97.45
2.86-359.2	110.5	129.3	3.63-43.98	25.08	13.10	19.61-335.6	157.8	94.05
33.64-3531	1229	1100	252.7-4141	1547	1415	1611-7522	2945	1375
108.6-200.3	151.6	35.11	79.56-628.4	193.1	171.8	68.49-258.2	130.7	53.50

colour and only rarely show colour zoning (DuToit 2012; Buathong & Narudeesombat 2020), in contrast to corundum, in which chemical and colour zoning are very common.

U-Pb Radiometric Dating

U-Pb dating of all four surface-reaching zircon inclusions analysed in two of the type 1 spinels yielded an

approximate age of 500 Ma (e.g. Figure 19). This is well in line with radiometric ages for zircon inclusions in rubies and sapphires from East Africa, Sri Lanka and Madagascar (Link 2015; Elmaleh *et al.* 2019; Krzemnicki *et al.* 2019) and can be linked to mineralisation during a late stage of the East African Orogeny (650–500 Ma). These inclusion analyses showed no mixed ages due to accidental ablation of an old detrital zircon core. We thus assume that the calculated U-Pb ages represent the formation age not only of the zircon but also of the spinel during the East African Orogeny, although complex internal zoning of zircon (e.g. an older detrital core) cannot be fully excluded.

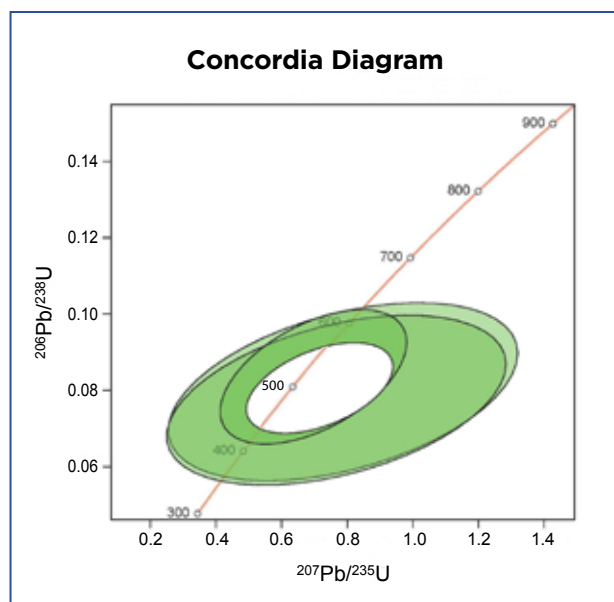


Figure 19: This Concordia diagram for zircon inclusions in a Co-bearing spinel from the Lukande area (SPTan-1_13) reveals an average (n = 3) U-Pb age of 501.1 ± 29.1 Ma. The 'concordia line' in the centre of the plot shows the U-Pb ratios for a closed system in which all the Pb originates from U decay (i.e. undisturbed by later events such as metamorphism). Figure by H. A. O. Wang, SSEF.

DISCUSSION

The new deposit in the Lukande area in Tanzania has produced a number of attractive blue spinels since September 2021. Our study of a selection of these stones reveals that they all contain traces of Co in various amounts, which has an impact not only on their colour but also on their commercial value. Various criteria have been used to assess whether a stone can be properly termed *Co-spinel* in the gem trade. The first and most strict example is limiting the term only to those spinels that show a vibrant, saturated blue colour resulting from the presence of Co. This excludes lighter blue spinels (e.g. from Vietnam), even though their colour is basically only due to traces of cobalt.

Another approach is to use concentrations of colouring elements, mainly cobalt and iron (e.g. >40–60 ppm Co in 'low-Fe' spinels; Peretti *et al.* 2015) or Co/Fe

(and Co/Cr) ratios (Sokolov *et al.* 2019; Schollenbruch *et al.* 2021). These approaches have some limitations, as they are based mainly on concentrations, and do not take into account the influence of iron on the absorption spectrum depending on its valence state (Fe^{2+} and Fe^{3+}) and site occupancy (octahedrally and tetrahedrally coordinated). Another drawback is that, in most cases, this approach requires LA-ICP-MS analysis, as Co usually cannot be detected by EDXRF.

The concept used by most gemmological laboratories is to rely mainly on the visible-range spectrum—which has to be dominated by cobalt absorption bands—in combination with the observed colour. This concept interprets the term *Co-spinel* as a gem varietal name (similar to corundum varieties such as sapphire, ruby or padparadscha), accepting a certain range of colour hues and saturations, as long as the above-mentioned criteria are met.

Our UV-Vis-NIR spectral analyses have clearly shown that this new Tanzanian source produces spinels gradually ranging from blue stones with an absorption spectrum dominated by Co (Figure 15: sample SPTan-1_12) to greyish-greenish blue material with Fe absorption dominating over the Co bands (Figure 15: sample SPTan-1_23; see also Chauviré *et al.* 2015). In this latter sample, the main absorption is greatest at 555 nm ($^{\text{T}}\text{Fe}^{2+}$), with a distinct shoulder at about 670 nm ($^{\text{M}}\text{Fe}^{2+}$ – $^{\text{M}}\text{Fe}^{3+}$ IVCT) and strong Fe peaks in the UV range ($^{\text{T}}\text{Fe}^{2+}$ and O^{2-} – Fe^{2+} LMCT). In the other two spectra in Figure 15, Co-related bands predominate in the visible range. This is also evident from the trace-element data

(see Figure 18 and Table III), which reveal a distinctly lower concentration of Co but higher Fe in the greyish-greenish blue spinel sample. As such, in our opinion not all blue spinels from this new deposit should be called *Co-spinel*, although all of them contain traces of Co to some extent.

Interestingly, Co-bearing spinels from this new source, but also from other origins, contain similar traces of Ni, as both of these elements are geochemically related. Nickel, commonly also present as Ni^{2+} , is assumed to replace tetrahedrally coordinated Mg^{2+} . Such $^{\text{T}}\text{Ni}^{2+}$ also results in a blue colour, but with a slightly more greenish hue (similar to ‘Swiss blue’ irradiated topaz) and lower saturation (Hanser 2013).

In a previous study on blue spinels, a Verneuil synthetic doped with Ni was investigated and compared to Co-spinel from Vietnam and also to synthetic Co-spinels (Hanser 2013). The spectrum of the Ni-doped sample showed two main absorption-band systems, the first in the UV centred at 377 nm, and the second a broad system centred at about 595 nm (Figure 20a). Interestingly, Co absorption is much stronger than Ni. This is evident in Figure 20b, which compares two Verneuil synthetic spinels, one doped with Ni (about 1100 ppm) and the other with Co (330 ppm). Consequently, we would not expect to see Ni-related absorption features in our natural spinel samples, even more so because Fe-related bands strongly overlap the positions of the Ni bands.

The geographic origin determination of spinel and, specifically, of Co-spinel, has become more important

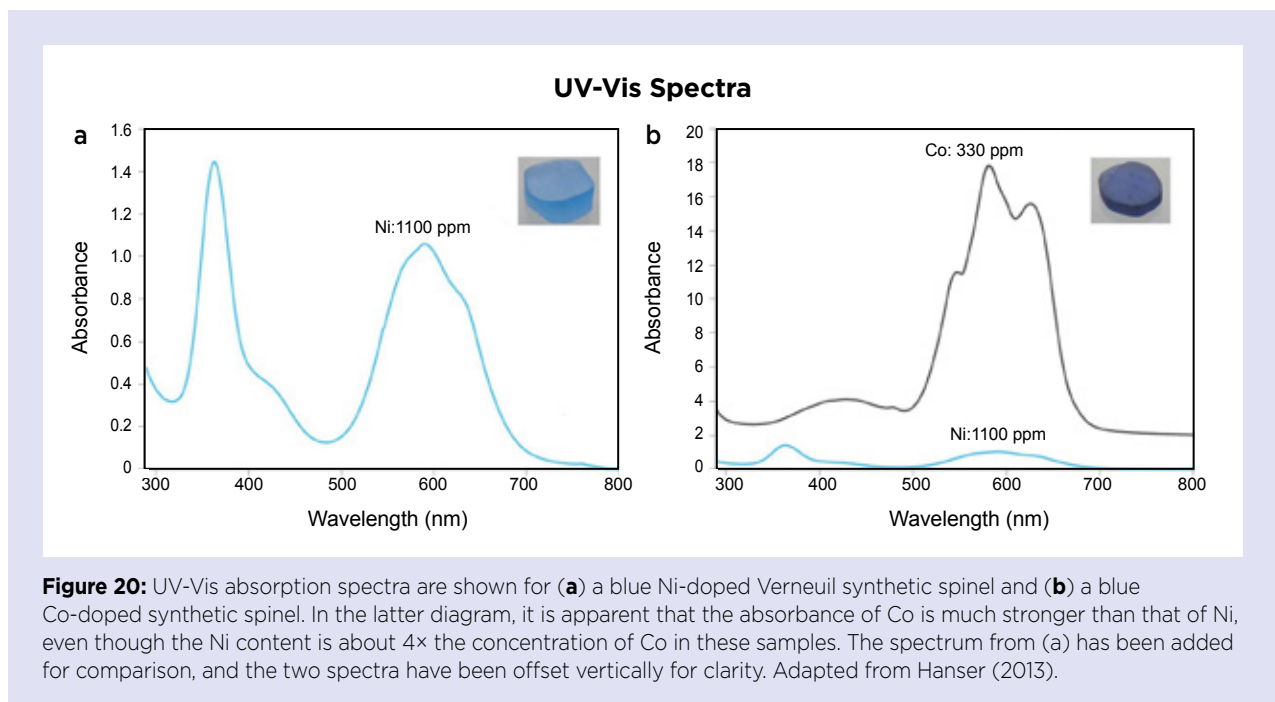


Figure 20: UV-Vis absorption spectra are shown for (a) a blue Ni-doped Verneuil synthetic spinel and (b) a blue Co-doped synthetic spinel. In the latter diagram, it is apparent that the absorbance of Co is much stronger than that of Ni, even though the Ni content is about 4× the concentration of Co in these samples. The spectrum from (a) has been added for comparison, and the two spectra have been offset vertically for clarity. Adapted from Hanser (2013).

for the trade in recent years. As mentioned above, our study has shown that Co-bearing spinel from Tanzania often shows characteristic inclusion features (högbomite lamellae), which could help gemmologists with origin determination.

In addition, trace elements are commonly used for the origin determination of coloured stones, including spinels. Figure 21 shows four different scatterplots (based on the data in Table III) comparing Ni, Mn, Fe and Ti with Co concentrations in Co-bearing spinels from Tanzania, Sri Lanka, Vietnam and Pakistan. Generally, Tanzanian type I spinels are quite uniform and can be separated from those of Pakistan by lower Co, Ni and Fe, as well as higher Mn. Tanzanian type I spinels can be further distinguished from those of Sri Lanka and Vietnam by different Ti contents. Sri Lankan samples seem to be very non-uniform. Plotting Co vs Ni (Figure 21a) reveals a general positive correlation for these elements ($r =$ approximately 1) in

slightly separate but overlapping fields for each locality, except for the Sri Lankan samples, which do not follow this general trend. By contrast, the Co vs Mn plot (Figure 21b) shows a slight negative correlation for these two transition elements. In a plot of Co vs Fe (Figure 21c), the Tanzanian type I spinel can be separated from a Pakistan origin by their lower Co and Fe contents. However, they show considerable overlap with Co and Fe for analysed samples from Vietnam and Sri Lanka.

Interestingly, the Tanzanian type I spinels in all four plots form a restricted and well-defined group. The scatterplots thus confirm that the analysed samples are chemically quite homogeneous, indeed much more so than gem-quality Co-bearing spinel from other origins, as seen also from the rather low standard-deviation values in Table III. In contrast to this, Tanzanian type II spinels plot in a much wider range, best fitting with Co-spinels from Pakistan.

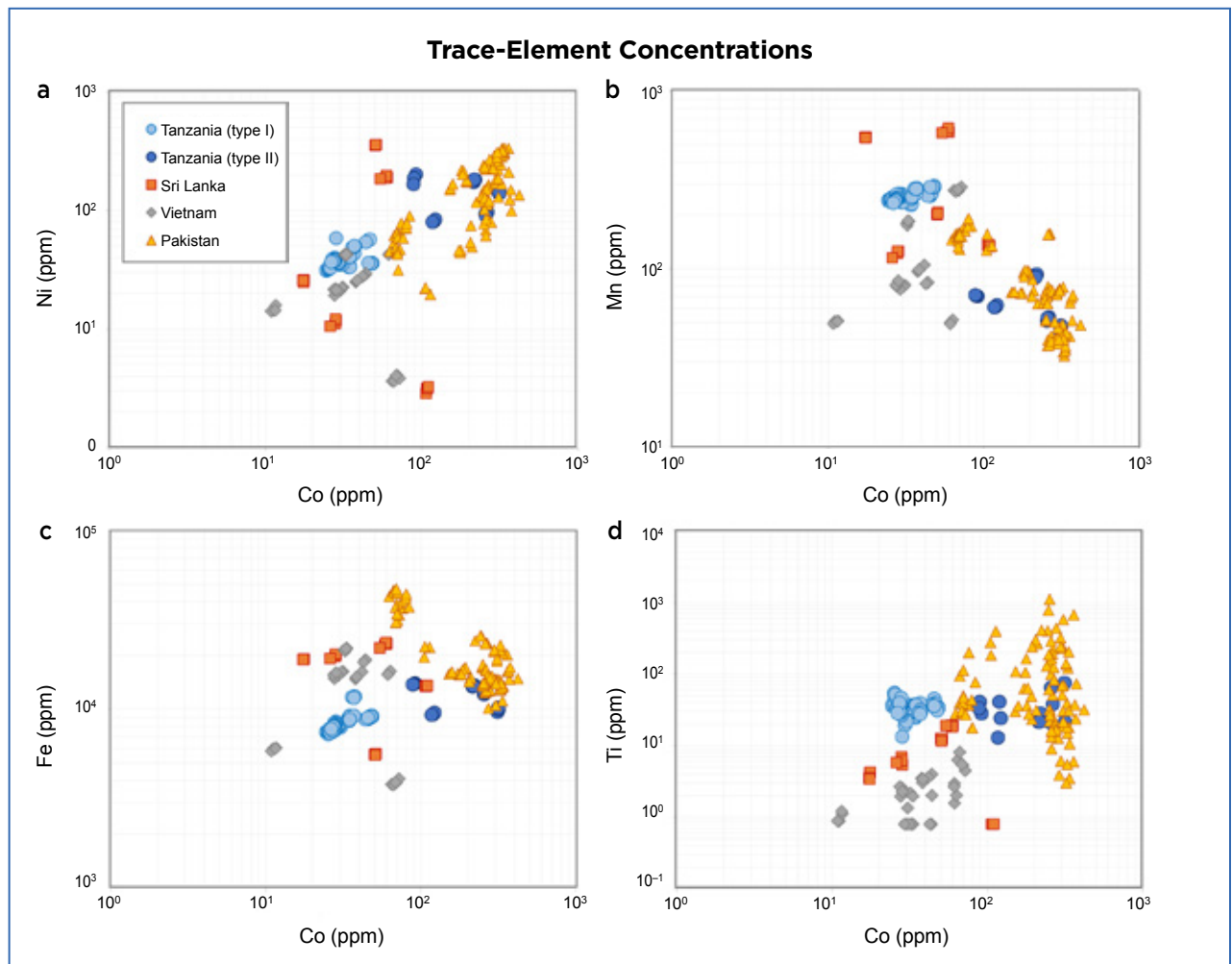


Figure 21: Trace-element plots are shown for Co-bearing spinel from Tanzania together with samples from Vietnam, Sri Lanka and Pakistan for: (a) Co vs Ni, (b) Co vs Mn, (c) Co vs Fe and (d) Co vs Ti. Error bars were calculated but found to be smaller than the data spots.

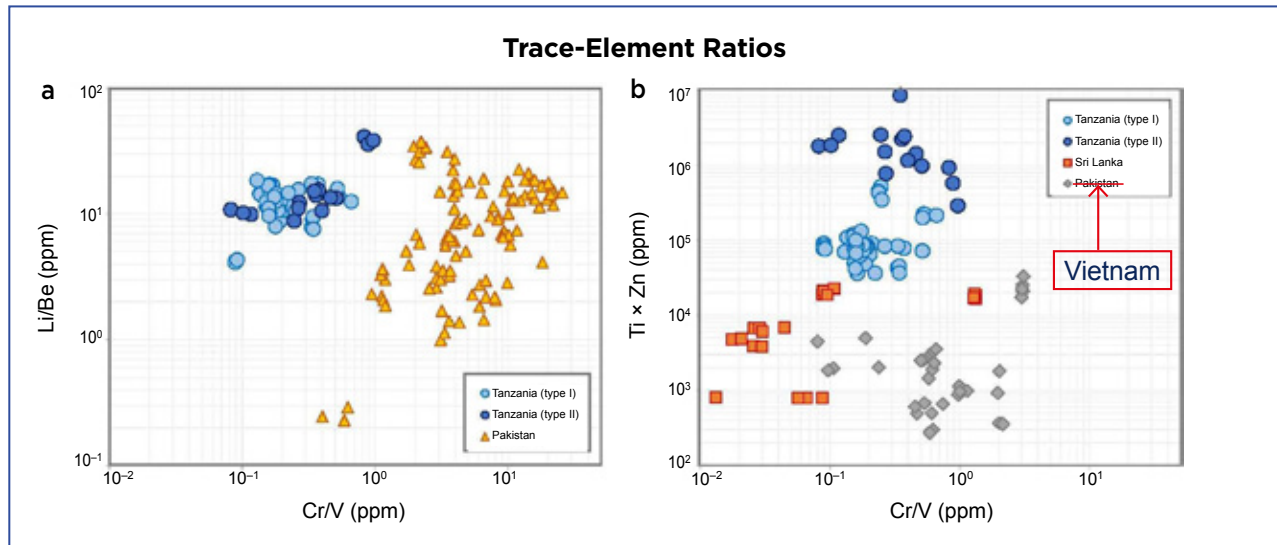


Figure 22: Plots of trace-element ratios are helpful for separating Tanzanian Co-bearing spinels from those of (a) Pakistan using Cr/V vs Li/Be, and (b) Vietnam and Sri Lanka using Cr/V vs Ti × Zn. Error bars were calculated but found to be smaller than the data spots.

Another approach to separating Co-bearing blue spinel from different origins is by using concentration-ratio plots (Figure 22). The analysed samples from Tanzania (types

I and II) can be well separated from Co-spinels from Pakistan by plotting Cr/V versus Li/Be (Figure 22a). Sri Lankan and Vietnamese samples overlap in this plot and therefore are not shown. However, by also using a plot of Cr/V versus Ti × Zn (Figure 22b), stones from Tanzania (types I and II) can be well separated from Vietnamese and Sri Lankan blue spinel.



Figure 23: This platinum ring features a 2.69 ct Tanzanian Co-bearing blue spinel that is set with smaller grey-to-blue spinels (2 ct total weight). Courtesy of Mary van der Aa Fine Jewels; stones faceted by Tucson Todd's Gems (Tucson, Arizona, USA).

CONCLUSIONS

A new deposit of Co-bearing blue spinel is associated with weathered marble in the Lukande area about 15 km south-east of Mahenge in central Tanzania. The stones first reached the market in September 2021, and they vary from attractive blue Co-spinel to greyish blue material dominated by Fe-related absorption bands in the visible spectral range. Some stones attain relatively large sizes, weighing up to 10+ ct, making this deposit an important newcomer to the global gem trade. The beauty of these Co-bearing blue spinels from Tanzania is the driving force for their desirability in jewellery (e.g. Figure 23).

The geological context, combined with field observations and U-Pb dating, indicate the formation of the deposit near Lukande is linked to late-stage metamorphic events of the EAO. This is well in line with other marble-hosted gem deposits in central Tanzania (i.e. ruby and spinel deposits in the Uluguru and Mahenge mountains). These new Co-bearing blue spinels from Tanzania can be separated from Co-spinels from Vietnam, Sri Lanka and Pakistan based on their characteristic inclusion features and trace-element patterns.

REFERENCES

- Abritta, T. & Blak, F.H. 1991. Luminescence study of $\text{ZnGa}_2\text{O}_4:\text{Co}^{2+}$. *Journal of Luminescence*, **48–49**(Part 2), 558–560, [https://doi.org/10.1016/0022-2313\(91\)90192-x](https://doi.org/10.1016/0022-2313(91)90192-x).
- Andreozzi, G.B., D’Ippolito, V., Skogby, H., Hålenius, U. & Bosi, F. 2018. Color mechanisms in spinel: A multi-analytical investigation of natural crystals with a wide range of coloration. *Physics and Chemistry of Minerals*, **46**(4), 343–360, <https://doi.org/10.1007/s00269-018-1007-5>.
- Balmer, W.A. 2011. *Petrology, geochemistry, and gemmological characterisation of marble-hosted ruby deposits of the Morogoro Region, Tanzania*. PhD thesis, Chulalongkorn University, Bangkok, Thailand, 185 pp.
- Balmer, W.A., Hauzenberger, C.A., Fritz, H. & Sutthirath, C. 2017. Marble-hosted ruby deposits of the Morogoro Region, Tanzania. *Journal of African Earth Sciences*, **134**, 626–643, <https://doi.org/10.1016/j.jafrearsci.2017.07.026>.
- Bank, H., Henn, U. & Petsch, E. 1989. Spinelle aus dem Umba-Tal, Tanzania. *Gemmologie: Zeitschrift der Deutschen Gemmologischen Gesellschaft*, **38**, 166–168.
- Belley, P.M. & Groat, L.A. 2019. Metacarbonate-hosted spinel on Baffin Island, Nunavut, Canada: Insights into the origin of gem spinel and cobalt-blue spinel. *Canadian Mineralogist*, **57**(2), 147–200, <https://doi.org/10.3749/canmin.1800060>.
- Birch, R.L. & Stephenson, E.A. 1962. *Geological Map Series of Tanganyika, Quarter Degree Sheet 251*. Directorate of Overseas Surveys, London.
- Bosi, F., Hålenius, U., D’Ippolito, V. & Andreozzi, G.B. 2012. Blue spinel crystals in the $\text{MgAl}_2\text{O}_4\text{-CoAl}_2\text{O}_4$ series: Part II. Cation ordering over short-range and long-range scales. *American Mineralogist*, **97**(11–12), 1834–1840, <https://doi.org/10.2138/am.2012.4139>.
- Branstrator, B. 2022. A new source in Tanzania is producing cobalt-blue spinel. *National Jeweler*, <https://nationaljeweler.com/articles/10908-a-new-source-in-tanzania-is-producing-cobalt-blue-spinel>, 17 May, accessed 28 February 2023.
- Buathong, A. & Narudeesombat, N. 2020. Gem Notes: A rare bicoloured spinel. *Journal of Gemmology*, **37**(3), 250–252, <https://doi.org/10.15506/JoG.2020.37.3.250>.
- Chauviré, B., Rondeau, B., Fritsch, E., Ressigeac, P. & Devidal, J.-L. 2015. Blue spinel from the Luc Yen District of Vietnam. *Gems & Gemology*, **51**(1), 2–17, <https://doi.org/10.5741/gems.51.1.2>.
- Cornu, L., Gaudon, M., Ilin, E., Aymonier, C., Veber, P., Garcia, A., Kahn, M., Champouret, Y. *et al.* 2015. Luminescence of sensitive materials: Towards new optical sensing. *Oxide-based Materials and Devices VI*, San Francisco, California, USA, 7–12 February, <https://doi.org/10.1117/12.2076948>.
- D’Ippolito, V., Andreozzi, G.B., Hålenius, U., Skogby, H., Hametner, K. & Günther, D. 2015. Color mechanisms in spinel: Cobalt and iron interplay for the blue color. *Physics and Chemistry of Minerals*, **42**(6), 431–439, <https://doi.org/10.1007/s00269-015-0734-0>.
- DuToit, G. 2012. Lab Notes: Bicolored spinel. *Gems & Gemology*, **48**(4), 304.
- Elmaleh, E., Schmidt, S.T., Karampelas, S., Link, K., Kiefert, L., Sussenberger, A. & Paul, A. 2019. U-Pb ages of zircon inclusions in sapphires from Ratnapura and Balangoda (Sri Lanka) and implications for geographic origin. *Gems & Gemology*, **55**(1), 18–28, <https://doi.org/10.5741/gems.55.1.18>.
- Fregola, R.A., Skogby, H., Bosi, F., D’Ippolito, V., Andreozzi, G.B. & Hålenius, U. 2014. Optical absorption spectroscopy study of the causes for color variations in natural Fe-bearing garnet: Insights from iron valency and site distribution data. *American Mineralogist*, **99**(11–12), 2187–2195, <https://doi.org/10.2138/am-2014-4962>.
- Fritz, H., Tenczer, V., Hauzenberger, C.A., Wallbrecher, E., Hoinkes, G., Muhongo, S. & Mogessie, A. 2005. Central Tanzanian tectonic map: A step forward to decipher Proterozoic structural events in the East African Orogen. *Tectonics*, **24**(6), article TC6013, <https://doi.org/10.1029/2005tc001796>.
- Fritz, H., Tenczer, V., Hauzenberger, C., Wallbrecher, E. & Muhongo, S. 2009. Hot granulite nappes – Tectonic styles and thermal evolution of the Proterozoic granulite belts in East Africa. *Tectonophysics*, **477**(3–4), 160–173, <https://doi.org/10.1016/j.tecto.2009.01.021>.
- Fritz, H., Abdelsalam, M., Ali, K.A., Bingen, B., Collins, A.S., Fowler, A.R., Ghebreab, W., Hauzenberger, C.A. *et al.* 2013. Orogen styles in the East African Orogen: A review of the Neoproterozoic to Cambrian tectonic evolution. *Journal of African Earth Sciences*, **86**, 65–106, <https://doi.org/10.1016/j.jafrearsci.2013.06.004>.
- Gaffney, E.S. 1973. Spectra of tetrahedral Fe^{2+} in MgAl_2O_4 . *Physical Review B*, **8**(7), 3484–3486, <https://doi.org/10.1103/PhysRevB.8.3484>.
- Gaft, M., Reisfeld, R. & Panczer, G. 2015. *Modern Luminescence Spectroscopy of Minerals and Materials*. Springer-Verlag, Berlin, Germany, 356 pp., <https://doi.org/10.1007/978-3-319-24765-6>.
- Hålenius, U., Skogby, H. & Andreozzi, G.B. 2002. Influence of cation distribution on the optical absorption spectra of Fe^{3+} -bearing spinel s.s.-hercynite crystals: Evidence for electron transitions in ${}^{\text{VI}}\text{Fe}^{2+}\text{-}{}^{\text{VI}}\text{Fe}^{3+}$ clusters. *Physics and Chemistry of Minerals*, **29**(5), 319–330, <https://doi.org/10.1007/s00269-002-0240-z>.

- Hänni, H.A. & Schmetzer, K. 1991. New rubies from the Morogoro area, Tanzania. *Gems & Gemology*, **27**(3), 156–167, <https://doi.org/10.5741/gems.27.3.156>.
- Hanser, C.S. 2013. *Blue spinel from Luc Yen, Vietnam: A spectroscopic study*. Bachelor's thesis, University of Freiburg, Freiburg im Breisgau, Germany, 52 pp.
- Hauzenberger, C.A., Sommer, H., Fritz, H., Bauernhofer, A., Kröner, A., Hoinkes, G., Wallbrecher, E. & Thöni, M. 2007. SHRIMP U–Pb zircon and Sm–Nd garnet ages from the granulite-facies basement of SE Kenya: Evidence for Neoproterozoic polycyclic assembly of the Mozambique Belt. *Journal of the Geological Society*, **164**(1), 189–201, <https://doi.org/10.1144/0016-76492005-081>.
- Hendy, A., Krüger, A., Pfarr, K., De Witte, J., Kibweja, A., Mwingira, U., Dujardin, J.-C., Post, R. *et al.* 2018. The blackfly vectors and transmission of *Onchocerca volvulus* in Mahenge, south eastern Tanzania. *Acta Tropica*, **181**, 50–59, <https://doi.org/10.1016/j.actatropica.2018.01.009>.
- Henn, U. & Milisenda, C.C. 1997. Neue Edelsteinvorkommen in Tansania: die Region Tunduru-Songea. *Gemmologie: Zeitschrift der Deutschen Gemmologischen Gesellschaft*, **46**(1), 29–43.
- Khaidukov, N.M., Brekhovskikh, M.N., Kirikova, N.Y., Kondratyuk, V.A. & Makhov, V.N. 2020. Luminescence properties of spinels doped with manganese ions. *Russian Journal of Inorganic Chemistry*, **65**(8), 1135–1141, <https://doi.org/10.1134/s0036023620080069>.
- Koivula, J.I., Kammerling, R.C. & Fritsch, E. 1993. Gem News: Ruby mining near Mahenge, Tanzania. *Gems & Gemology*, **29**(2), 136.
- Krzemnicki, M.S. 2022. SSEF conducts analysis of cobalt-blue spinel from a newly reported source in Tanzania. Swiss Gemmological Institute SSEF, 2 pp., <https://tinyurl.com/2p92wxjp>, 16 May, accessed 28 February 2023.
- Krzemnicki, M.S., Wang, H.A.O. & Phyo, M.M. 2019. Age dating applied as a testing procedure to gemstones and biogenic gem materials. *36th International Gemmological Conference*, Nantes, France, 28–31 August, 48–50, <https://tinyurl.com/52x8xrdb>.
- Kukharuk, M. & Manna, C. 2019. The spinels of Mahenge, Tanzania. *InColor*, No. 43, 54–58, <http://www.incolormagazine.com/books/robz/#p=54>.
- Kuleshov, N.V., Mikhailov, V.P., Scherbitsky, V.G., Prokoshin, P.V. & Yumashev, K.V. 1993. Absorption and luminescence of tetrahedral Co^{2+} ion in MgAl_2O_4 . *Journal of Luminescence*, **55**(5–6), 265–269, [https://doi.org/10.1016/0022-2313\(93\)90021-e](https://doi.org/10.1016/0022-2313(93)90021-e).
- Link, K. 2015. Age determination of zircon inclusions in faceted sapphires. *Journal of Gemmology*, **34**(8), 692–700, <https://doi.org/10.15506/JoG.2015.34.8.692>.
- Marfunin, A.S. 1979. *Physics of Minerals and Inorganic Materials*. Springer-Verlag, Berlin, Germany, xii + 342 pp.
- Meert, J.G. 2003. A synopsis of events related to the assembly of eastern Gondwana. *Tectonophysics*, **362**(1–4), 1–40, [https://doi.org/10.1016/s0040-1951\(02\)00629-7](https://doi.org/10.1016/s0040-1951(02)00629-7).
- Möller, A., Mezger, K. & Schenk, V. 2000. U–Pb dating of metamorphic minerals: Pan-African metamorphism and prolonged slow cooling of high pressure granulites in Tanzania, East Africa. *Precambrian Research*, **104**(3–4), 123–146, [https://doi.org/10.1016/s0301-9268\(00\)00086-3](https://doi.org/10.1016/s0301-9268(00)00086-3).
- Nasdala, L., Irmer, G. & Wolf, D. 1995. The degree of metamictization in zircon: A Raman spectroscopic study. *European Journal of Mineralogy*, **7**(3), 471–478, <https://doi.org/10.1127/ejm/7/3/0471>.
- Pardieu, V. & Hughes, R.W. 2008. Spinel: Resurrection of a classic. *InColor*, No. 8, 10–18, <http://www.incolormagazine.com/books/gibu/#p=10>.
- Peretti, A., Günther, D. & Haris, M.T.M. 2015. GRS Alert: New spinel treatment discovered involving heat and cobalt-diffusion. GRS Gemresearch Swisslab, 4 pp., <https://tinyurl.com/2kdau95s>, 22 May, accessed 28 February 2023.
- Phyo, M.M., Wang, H.A.O., Guillong, M., Berger, A., Franz, L., Balmer, W.A. & Krzemnicki, M.S. 2020. U–Pb dating of zircon and zirconolite inclusions in marble-hosted gem-quality ruby and spinel from Mogok, Myanmar. *Minerals*, **10**(2), article 195, <https://doi.org/10.3390/min10020195>.
- Quinn, E.P. & Laurs, B.M. 2004. Gem News: Pink to pink-orange spinel from Tanzania. *Gems & Gemology*, **40**(1), 71–72.
- Rossetti, F., Cozzupoli, D. & Phillips, D. 2008. Compressional reworking of the East African Orogen in the Uluguru Mountains of eastern Tanzania at c. 550 Ma: Implications for the final assembly of Gondwana. *Terra Nova*, **20**(1), 59–67, <https://doi.org/10.1111/j.1365-3121.2007.00787.x>.
- Saeseaw, S., Wang, W., Scarratt, K., Emmett, J.L. & Douthit, T.R. 2009. Distinguishing heated spinels from unheated natural spinels and from synthetic spinels: A short review of on-going research. Gemological Institute of America, 13 pp., <https://www.gia.edu/doc/Heated-spinel-Identification-at-April-02-2009.pdf>, 2 April, accessed 28 February 2023.
- Sampson, D.N. & Wright, A.E. 1964. *The Geology of the Uluguru Mountains*. Government Printer, Dar es Salaam, Tanzania, 69 pp.
- Schaub, P. 2004. *Spektrometrische Untersuchungen an Al–Spinellen*. Master's thesis, University of Basel, Switzerland, 275 pp.

- Schlüter, T. 1997. *Geology of East Africa*. Gebrüder Borntraeger, Berlin, Germany, xii + 484 pp.
- Schmetzer, K. & Berger, A. 1992. Lamellar inclusions in spinels from Morogoro area, Tanzania. *Journal of Gemmology*, **23**(2), 93–94, <https://doi.org/10.15506/JoG.1992.23.2.93>.
- Schmetzer, K., Haxel, C. & Amthauer, G. 1989. Colour of natural spinels, gahnospinel and gahnites. *Neues Jahrbuch für Mineralogie, Abhandlungen*, **160**(2), 159–180.
- Schollenbruch, K., Malsy, A.-K., Bosshard, V. & Blauwet, D. 2021. Cobalt-blue spinel from northern Pakistan. *Journal of Gemmology*, **37**(7), 726–737, <https://doi.org/10.15506/JoG.2021.37.7.726>.
- Schwarz, D., Liu, Y., Zhou, Z., Lomthong, P. & Rozet, T. 2022. Spinel from the Pamir Mountains in Tajikistan. *Journal of Gemmology*, **38**(2), 138–154, <https://doi.org/10.15506/JoG.2022.38.2.138>.
- Shigley, J.E. & Stockton, C.M. 1984. ‘Cobalt-blue’ gem spinels. *Gems & Gemology*, **20**(1), 34–41, <https://doi.org/10.5741/gems.20.1.34>.
- Smith, C.P., Beesley, C.R., Quinn Darenius, E., Mayerson, W.M. 2008. A closer look at Vietnamese spinel. *InColor*, No. 43, 31–34, <http://www.incolormagazine.com/books/kvfr/#p=10>.
- Smith, C.P. 2012. Spinel and its treatments: A current status report. *InColor*, No. 19, 50–54, <http://www.incolormagazine.com/books/pcpz/#p=50>.
- Sokolov, P., Kuksa, K., Marakhovskaya, O. & Gussiås, G.A. 2019. In search of cobalt blue spinel in Vietnam. *InColor*, No. 43, 60–65, <http://www.incolormagazine.com/books/robz/#p=60>.
- Stephan, T., Henn, U. & Muller, S. 2022. Neue Funde von kobalthaltigem Spinel bei Mahenge, Tansania. *Gemmologie: Zeitschrift der Deutschen Gemmologischen Gesellschaft*, **71**(3/4), 57–64.
- Stern, R.J. 1994. Arc assembly and continental collision in the Neoproterozoic East African Orogen: Implications for the consolidation of Gondwanaland. *Annual Review of Earth and Planetary Sciences*, **22**(1), 319–351, <https://doi.org/10.1146/annurev.ea.22.050194.001535>.
- Taran, M.N., Koch-Müller, M. & Langer, K. 2005. Electronic absorption spectroscopy of natural (Fe²⁺, Fe³⁺)-bearing spinels of spinel s.s.-hercynite and gahnite-hercynite solid solutions at different temperatures and high-pressures. *Physics and Chemistry of Minerals*, **32**(3), 175–188, <https://doi.org/10.1007/s00269-005-0461-z>.
- Taran, M.N., Koch-Müller, M. & Feenstra, A. 2009. Optical spectroscopic study of tetrahedrally coordinated Co²⁺ in natural spinel and staurolite at different temperatures and pressures. *American Mineralogist*, **94**(11–12), 1647–1652, <https://doi.org/10.2138/am.2009.3247>.
- Wang, H.A.O. & Krzemnicki, M.S. 2021. Multi-element analysis of minerals using laser ablation inductively coupled plasma time of flight mass spectrometry and geochemical data visualization using t-distributed stochastic neighbor embedding: Case study on emeralds. *Journal of Analytical Atomic Spectrometry*, **36**(3), 518–527, <https://doi.org/10.1039/d0ja00484g>.
- Wang, H.A.O., Krzemnicki, M.S., Chalain, J.-P., Lefèvre, P., Zhou, W. & Cartier, L. 2016. Simultaneous high sensitivity trace-element and isotopic analysis of gemstones using laser ablation inductively coupled plasma time-of-flight mass spectrometry. *Journal of Gemmology*, **35**(3), 212–223, <https://doi.org/10.15506/JoG.2016.35.3.212>.
- Weinberg, D. 2007. Giant red spinel crystal discovered in East Africa. Multicolour Gems Ltd, <https://www.multicolour.com/spinel/giant-red-spinel-crystal-discovered-in-east-africa.html>, 5 October, accessed 28 February 2023.
- Widmer, R., Malsy, A.-K. & Armbruster, T. 2014. Effects of heat treatment on red gemstone spinel: Single-crystal X-ray, Raman, and photoluminescence study. *Physics and Chemistry of Minerals*, **42**(4), 251–260, <https://doi.org/10.1007/s00269-014-0716-7>.
- Yu, C.F. & Lin, P. 1996. Manganese-activated luminescence in ZnGa₂O₄. *Journal of Applied Physics*, **79**(9), 7191–7197, <https://doi.org/10.1063/1.361435>.

The Authors

Dr Michael S. Krzemnicki^{FGA^{1,2,*}},
Alex Leuenberger³ and **Dr Walter A. Balmer**¹

¹ Swiss Gemmological Institute SSEF,
Aeschengraben 26, 4051 Basel, Switzerland

² Department of Environmental Sciences,
Mineralogy and Petrology, University of Basel,
Bernoullistrasse 32, 4056 Basel, Switzerland

³ ALine GmbH, Bernstrasse 264,
3627 Heimberg, Switzerland

* Email: michael.krzemnicki@ssef.ch

Acknowledgements

The authors thank the following gem traders for information and samples: Salim Almas (Arusha, Tanzania), Mark Saul (Swala Gem Traders Ltd, Arusha), Steve Jaquith (G.E.O. International Co. Ltd, Bangkok) and Wez Barber (Mahenge Gems Pte. Ltd, Singapore). Furthermore, we thank Dr Klaus Schollenbruch (Gübelin Gem Lab, Lucerne, Switzerland) for kindly providing LA-ICP-MS data of Co-bearing spinel from Pakistan. And finally, we thank the following people for data acquisition and processing at the Swiss Gemmological Institute SSEF: Dr H. A. O. Wang, Dr Markus Wälle, Judith Braun, Susanne Büche, Hannah Amsler and all other colleagues at SSEF for fruitful discussions.